

## Regular and Chaotic Chemical Spatiotemporal Patterns

W. Y. Tam, John A. Vastano, Harry L. Swinney, and W. Horsthemke<sup>(a)</sup>

Center for Nonlinear Dynamics and Department of Physics, The University of Texas, Austin, Texas 78712

(Received 18 August 1988)

The first experimental observation of a bifurcation sequence of patterns in a reaction-diffusion system is reported. The experiment on a one-dimensional system, maintained away from equilibrium, reveals steady, periodic, quasiperiodic, frequency-locked, period-doubled, and chaotic spatiotemporal states. Results from a model reaction-diffusion system agree qualitatively with the experiment and provide insight into the physical mechanism that drives the observed behavior.

PACS numbers: 05.45.+b, 05.70.Ln, 82.20.Wt

Spatiotemporal patterns are a ubiquitous feature of natural systems. Examples range from banded patterns in rocks to excitation waves across the heart to the epitome of pattern formation, embryogenesis. The mechanisms of pattern formation are often chemical in origin. In contrast to natural systems, laboratory experiments on chemical spatial pattern formation were until recently conducted in *closed* systems,<sup>1</sup> not in *open* chemostats such as those usually employed in the study of temporal structures.<sup>2</sup> Thus the observed patterns decay irreversibly and uncontrollably as thermodynamic equilibrium was approached. This problem can be overcome with the use of open reactors that have an external feed of reagents, so that spatiotemporal patterns can be sustained indefinitely.<sup>3</sup> Open reactors provide a second crucial advantage: Feed rates and feed concentrations can be used as control parameters to investigate bifurcation sequences.

In this Letter we study a new type of spatially extended open chemical system, the Couette reactor.<sup>4,5</sup> This is an effectively one-dimensional reaction-diffusion system with well-defined boundary conditions. Using a Belousov-Zhabotinskii reaction,<sup>6</sup> we have observed the bifurcation sequence shown in Fig. 1(a) as the feed rate of one of the species was varied. The essential features of the experimental observations are captured by a simple one-dimensional reaction-diffusion model with a skeletal scheme<sup>7</sup> for the Belousov-Zhabotinskii chemistry.<sup>8</sup> Numerical studies of the model yield a bifurcation sequence leading to chaos that is in qualitative agreement with the sequence observed in the experiment, as can be seen by comparing Fig. 1(a) with 1(b).

We will first describe the experimental setup and the numerical model and then discuss the results further. The Couette reactor consists of two concentric cylinders with the inner cylinder rotating and the outer cylinder at rest (see Fig. 2). Reagents of the Belousov-Zhabotinskii reaction are fed into the cylindrical annulus with the oxidizer (bromate) at one end of the reactor and the reducer (glucose) at the other end.<sup>6</sup> The rate of removal of chemicals at each end is carefully adjusted to match the feed rate; thus there is *no* net axial flow. Experiments

indicate that the transport arising from the hydrodynamic flow can be modeled as a one-dimensional diffusion process in the axial direction; the effective axial diffusion coefficient is about  $0.08 \text{ cm}^2/\text{s}$  at the 6-Hz cylinder rotation rate used in the present experiment.<sup>9</sup> In each run the same hydrodynamic state is produced by use of a slow, programmed acceleration of the inner cylinder from rest to the final rotation rate.

We model the chemistry in the Couette reactor using the two-variable Oregonator kinetics; the variables are the concentrations  $u$  and  $v$  of the bromous acid and the catalyst, respectively.<sup>7</sup> The kinetic equations also include bromate (labeled  $A$ ) and the organic substrate (labeled  $B$ ), but  $A$  and  $B$  are held fixed in numerical studies of well-stirred reactors since they do not vary much in one oscillation of the reaction. For the Couette reactor

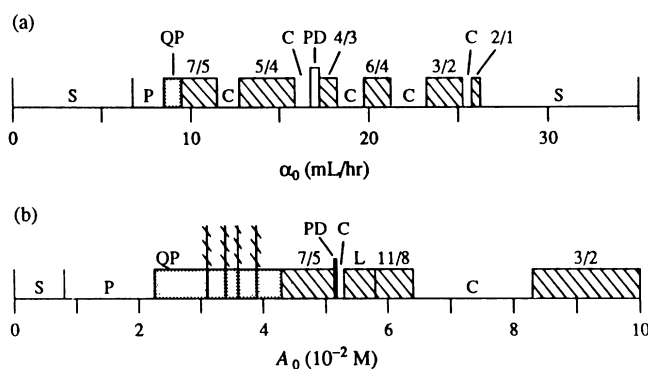


FIG. 1. (a) Bifurcation sequence obtained in the experiment, where the control parameter is  $\alpha_0$ , the bromate feed rate. (b) Bifurcation sequence for the model, where the control parameter is  $A_0$ , the bromate feed concentration. The observed spatiotemporal patterns are steady (S), periodic (P), quasiperiodic (QP), frequency locked, period doubled (PD), and chaotic (C); some attractors corresponding to these states are illustrated in Fig. 3. Frequency-locked states are labeled by the frequency-locking ratio, except for a region labeled L in (b), where there are many different frequency-locked states, and the hatched vertical lines in (b), which are very narrow windows of frequency-locked states.

this translates into the assumption that the spatial concentration profiles of  $A$  and  $B$  are determined solely by diffusion and hence vary linearly with axial position. The final model equations in dimensionless form are

$$\partial_t u = D \partial_{zz} u + (1/\varepsilon) \{u[A(z) - u] + q(z)B(z)v[pA(z) - u]/[pA(z) + u]\}, \quad \partial_t v = D \partial_{zz} v + A(z)u - B(z)v,$$

with no-flux boundary conditions at  $z=0$  and  $z=1$ . The effective diffusion coefficient  $D$  is the same for both  $u$  and  $v$ . The stoichiometric factors  $\varepsilon$  and  $p$  are constants, and the factor  $q$  is assumed to have a linear spatial profile.<sup>10</sup> The experiment is modeled by feeding  $A$  at  $z=0$  and  $B$  at  $z=1$  with  $A_1 \equiv A(1) = A_0/6$ ,  $B_0 \equiv B(0) = B_1/6$ ,  $q(0) = 1.5$ , and  $q(1) = 0.9$ . We set  $D = 3.75 \times 10^{-4}$  (in dimensional form,  $D = 0.078$  cm<sup>2</sup>/s for a reactor of length 14.4 cm),  $\varepsilon = 2.2 \times 10^{-2}$ ,  $p = 3.5 \times 10^{-3}$ , and  $B_1 = 0.85$ . Our control parameter is  $A_0$ , the feed concentration of the bromate at the  $z=0$  end of the reactor.<sup>11</sup> The model equations were integrated numerically with use of second-order centered differencing on an equally spaced grid of 100 spatial sites to approximate the spatial derivatives.<sup>12</sup> The resulting set of ordinary differential equations was time stepped with a variable-step-size Gear-type integrator.

The dynamics of the spatiotemporal patterns observed in the experiment and the model were identified by examining phase portraits such as those shown in Fig. 3 for periodic, quasiperiodic, frequency-locked, and chaotic states.<sup>13</sup> A quasiperiodic state consists of two incommensurate frequencies; in a frequency-locked state these frequencies are locked at some rational ratio. Period doubling of frequency-locked states to chaotic states was observed in both the experiment and the model. In the model several such period-doubling sequences have been found (one is indicated in Fig. 1), while in the experi-

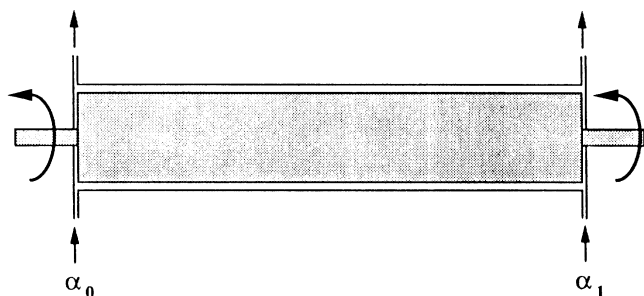


FIG. 2. The concentric-cylinder Couette reactor was mounted horizontally in a temperature-controlled bath ( $26.5 \pm 0.5^\circ\text{C}$ ). The inner (outer) cylinder radius was 1.093 cm (1.270 cm); the annulus length was 14.434 cm, which gave a fluid-height-to-gap ratio of 81.5. The bifurcation sequence was studied by varying the feed rate at  $z=0$ ,  $\alpha_0$ , from 0 to 35 ml/h; the feed contained 0.02M KBrO<sub>3</sub> and 1.0M H<sub>2</sub>SO<sub>4</sub>. The feed rate at  $z=1$ ,  $\alpha_1$ , was fixed (10 ml/h); that feed contained 0.1M glucose, 0.06M acetone, 0.002M MnSO<sub>4</sub>, and 1.0M H<sub>2</sub>SO<sub>4</sub>. The concentration of one of the intermediate species, bromide ion, was measured with sixteen ion-selective electrodes (Ag-AgBr) spaced equally along the axial extent of the reactor.

ment only one period-doubling sequence has been observed thus far.

The chaotic spatiotemporal patterns observed in both the experiment and the model are low dimensional. For example, the experimental chaotic attractor in Fig. 3(d) has a dimension of 2.1, and the Lyapunov spectrum<sup>14</sup> computed for the model (which has 200 variables—2 species at each of the 100 sites) shows that the dimension for the entire reaction-diffusion system is never greater than 2.4.

The frequencies of motion associated with a particular

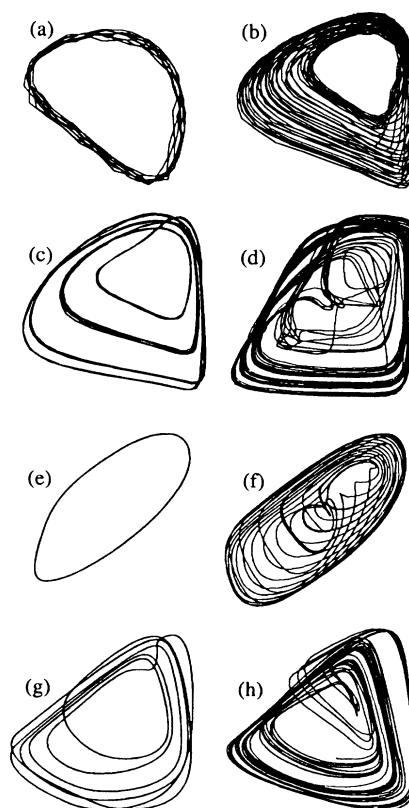


FIG. 3. (a)–(d) Attractors constructed from experimental measurements at  $z=0.20$  for  $\alpha_0 = 8.0, 9.0, 10.0,$  and  $16.0$  ml/h, respectively (Ref. 13). (e)–(h) Attractors from the model at  $z=0.25$  for  $A_0 = 0.020M, 0.025M, 0.050M,$  and  $0.065M$ , respectively. The attractors in (a) and (e) are limit cycles; (b),(f) 2-tori; (c),(g) frequency-locked  $\frac{1}{2}$  limit cycles; and (d),(h) chaotic attractors. In (a) the amplitude is 10 times smaller than in (b)–(d), and the spread of the limit cycle is due to experimental noise. The temporal behavior is the same at all spatial sites, although the amplitude varies with position, as Fig. 4 illustrates.

state are not seen at all spatial sites with the same amplitude, as Fig. 4 illustrates. The time series shown were taken at different spatial sites for a  $\frac{7}{5}$  frequency-locked state observed in the experiment [Figs. 4(a)–4(c)] and in the model [Fig. 4(d)–4(f)]. In the experiment, one frequency of motion,  $\omega_0$ , is observed close to the  $z=0$  end, and the other,  $\omega_1 = \frac{7}{5}\omega_0$ , is observed close to the  $z=1$  end. In the model, both frequencies can be observed at *any* position because of the high numerical precision, but the power at  $\omega_0$  decreases exponentially with  $z$  while the power at  $\omega_1$  increases exponentially with  $z$ . The spatio-temporal evolution of the  $\frac{7}{5}$  frequency-locked state observed in the experiment and in the model is presented in Fig. 5. The correspondence between the experiment and the reaction-diffusion model is remarkable.

The bifurcation sequence in Fig. 1 is typical of a single, periodically forced oscillator<sup>15</sup>: Steady-state behavior is followed by periodic oscillations, quasiperiodicity, frequency locking, and then chaos. The results from our

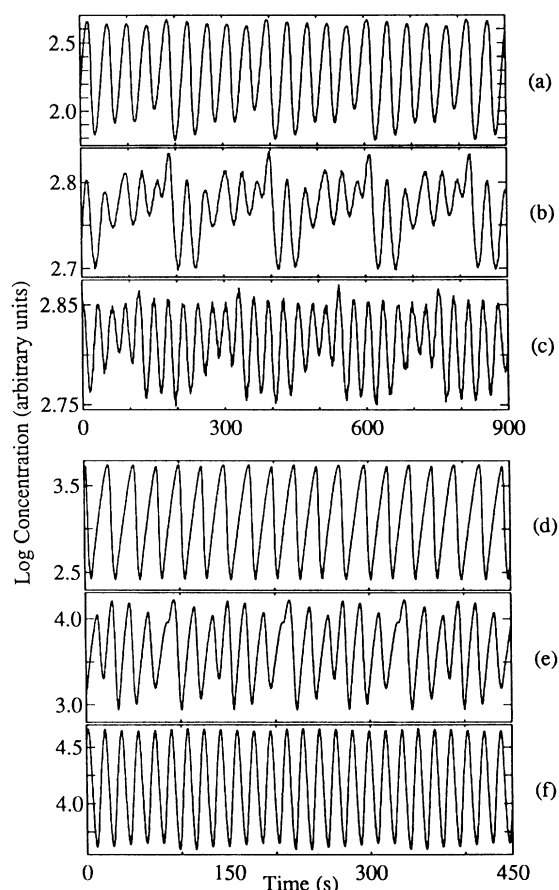


FIG. 4. The spatial variation of the dynamics for a  $\frac{7}{5}$  frequency-locked state: (a)–(c) time series of the logarithm of bromide-ion concentration measured at  $z=0.20$ ,  $0.40$ , and  $0.67$ , respectively ( $\alpha_0=10.0$  ml/h), and (d)–(f) time series of the logarithm of the model variable  $v(z,t)$  computed for  $z=0$ ,  $0.25$ , and  $0.50$ , respectively ( $A_0=0.050M$ ).

experiment and model indicate that in the reaction-diffusion system, diffusion averages the local kinetics to create, in effect, two oscillators localized near the two ends of the reactor. The mechanism can be understood from a consideration of the *local* (i.e.,  $D=0$ ) solutions for the kinetics. In the range of  $A_0$  for which our model system oscillates, the stable local solutions are periodic, and there is a spatial profile  $\omega_{loc}(z)$  of *local* frequencies. It has been shown analytically that if  $\omega_{loc}(z)$  is linear, then there is a solution for the reaction-diffusion system that oscillates at  $\langle\omega_{loc}(z)\rangle$ , the average frequency of the profile.<sup>16</sup> Although the frequency profile in our model system is not linear, this averaging mechanism is still important. The frequency  $\omega_0$  at the bromate end of the reaction-diffusion system is initially well approximated by  $\langle\omega_{loc}(z)\rangle$ , but as  $A_0$  is increased towards the bifurcation to quasiperiodicity, the approximation fails. At this point the frequency profile of the local kinetics in the model has developed a maximum near the middle of the reactor. We take this into account by defining  $\langle\omega_{loc}(z)\rangle_0$  and  $\langle\omega_{loc}(z)\rangle_1$  to be the spatially averaged frequencies on each side of the maximum. The frequency  $\omega_1$  of the oscillator localized near  $z=1$  is near  $\langle\omega_{loc}(z)\rangle_1$  for the entire range of  $A_0$  that we studied; in other words, it is given by the averaged local kinetics. In contrast,  $\omega_0$  is not well approximated by  $\langle\omega_{loc}(z)\rangle_0$ , as a result of the forcing by the oscillator near  $z=1$ . This diffusion-mediated interaction of two localized oscillators produces the observed bifurcation sequence to low-dimensional spatiotemporal chaos in our model. The good correspondence between the bifurcation sequences of the experiment and the model suggests that a similar process is occurring in the experiment.

Thus, the experimental and the model studies reveal that diffusive coupling of chemical kinetics with spatial gradients can generate complex behavior, including spa-

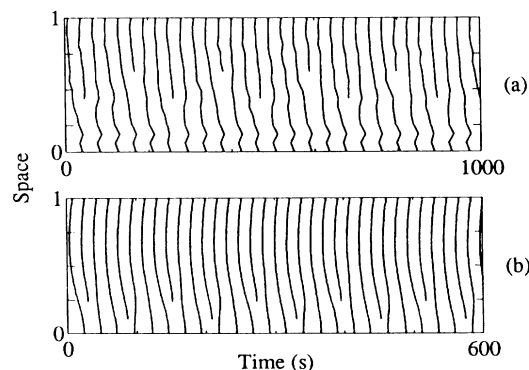


FIG. 5. Locations of local temporal maxima of a  $\frac{7}{5}$  frequency-locked state obtained from (a) the experiment for  $\alpha_0=10.0$  ml/h and (b) the model for  $A_0=0.050M$ . The lines clearly show the transition from a wave form with five maxima per period at  $z=0$  to one with seven maxima per period at  $z=1$ .

tiotemporal chaos, in a one-dimensional reaction-diffusion system maintained away from equilibrium. The bifurcation sequence of chemical spatiotemporal patterns from steady to low-dimensional chaotic behavior resembles that of a periodically forced nonlinear oscillator. A simple model of the chemistry, not intended to account for the details of the experimental system, reproduces the qualitative features of the bifurcation sequence leading to chaos in the Couette reactor<sup>11</sup> and provides an understanding of the mechanism underlying the observed phenomena.

We thank T. Russo and E. Kostelich for assistance, and P. DeKepper and Z. Noszticzius for valuable discussions. This work is a part of a research program supported by the BP Venture Research Unit and conducted in collaboration with P. DeKepper, J. C. Roux, and J. Boissonade, Centre de Recherche Paul Pascal, Bordeaux. Computing resources for this work were provided by the University of Texas Center for High Performance Computing.

(a)Present address: Department of Chemistry, Southern Methodist University, Dallas, TX 75275.

<sup>1</sup>See, e.g., J. Ross, S. C. Müller, and C. Vidal, *Science* **240**, 460 (1988); K. I. Agladze, A. V. Panfilov, and A. N. Rudenko, *Physica (Amsterdam)* **29D**, 409 (1988); C. Vidal, *J. Stat. Phys.* **48**, 1017 (1987); S. C. Müller, T. Plesser, and B. Hess, *Science* **230**, 661 (1985); B. J. Welsh, J. Gomatan, and A. E. Burgess, *Nature (London)* **304**, 611 (1983); A. T. Winfree, *Science* **175**, 634 (1972).

<sup>2</sup>F. Argoul, A. Arneodo, P. Richetti, J. C. Roux, and H. L. Swinney, *Acc. Chem. Res.* **20**, 436 (1987).

<sup>3</sup>Z. Noszticzius, W. Horsthemke, W. D. McCormick, H. L. Swinney, and W. Y. Tam, *Nature (London)* **329**, 619 (1987); W. Y. Tam, W. Horsthemke, Z. Noszticzius, and H. L. Swinney, *J. Chem. Phys.* **88**, 3395 (1988).

<sup>4</sup>J. B. Grutzner, E. A. Patrick, P. J. Pellechia, and M. Vera [*J. Am. Chem. Soc.* **110**, 726 (1988)] have studied simple acid-base and oxidation reactions in a closed Couette reactor.

<sup>5</sup>A concurrent study with an emphasis on stationary patterns

in a Couette reactor (using chlorite-iodide-malonic-acid chemistry) has been conducted by our collaborators, Q. Ouyang, J. Boissonade, J. C. Roux, and P. DeKepper (to be published).

<sup>6</sup>The dual substrate glucose-acetone was used in the Belousov-Zhabotinskii reaction instead of the usual malonic-acid substrate because the reaction with malonic acid produces gas bubbles that interfere with the spatial pattern and change the effective diffusion coefficient. In contrast, an insignificant amount of gas is produced by the glucose-acetone system. See Q. Ouyang, W. Y. Tam, P. DeKepper, W. D. McCormick, Z. Noszticzius, and H. L. Swinney, *J. Phys. Chem.* **91**, 2181 (1987).

<sup>7</sup>J. J. Tyson and P. C. Fife, *J. Chem. Phys.* **73**, 2224 (1980).

<sup>8</sup>R. J. Field and R. M. Noyes, *J. Chem. Phys.* **60**, 1877 (1974).

<sup>9</sup>W. Y. Tam and H. L. Swinney, *Phys. Rev. A* **36**, 1374 (1987).

<sup>10</sup>This is due to the spatial variation of  $A$  and  $B$  (P. DeKepper, private communication).

<sup>11</sup>The Oregonator model (Ref. 8), like most other chemical models, takes the feeds of open reactors into account in a simplified way: The concentrations of some reactants are fixed at the feed value. Thus the feed rate is not a control parameter in these models. The Oregonator model adequately describes an open system at low and moderate feed rates, but not at high feed rates. Thus the sequences in Fig. 1 differ for high values of the control parameters.

<sup>12</sup>Numerical studies with 50, 100, 200, and 500 sites yielded essentially the same bifurcation sequence, except for shifts of at most a few percent in the values of  $A_0$  at the bifurcations. See J. A. Vastano, Ph.D. dissertation, The University of Texas at Austin, 1988 (unpublished).

<sup>13</sup>The optimum time delays for the construction of the attractors were chosen by the method of A. M. Fraser and H. L. Swinney, *Phys. Rev. A* **33**, 1134 (1986).

<sup>14</sup>J. Kaplan and J. Yorke, in *Functional Differential Equations and the Approximation of Fixed Points*, edited by H. O. Peitgen and H. O. Walther, Lecture Notes in Mathematics Vol. 730 (Springer-Verlag, Berlin, 1979), p. 228.

<sup>15</sup>See, e.g., R. S. MacKay and C. Tresser, *Physica (Amsterdam)* **19D**, 206 (1986).

<sup>16</sup>G. B. Ermentrout and W. C. Troy, *SIAM J. Appl. Math.* **46**, 359 (1986).

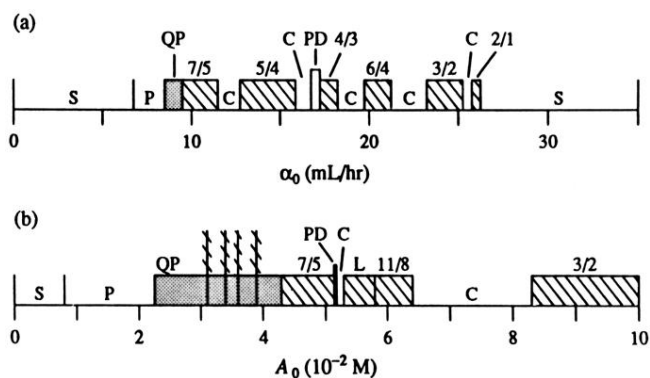


FIG. 1. (a) Bifurcation sequence obtained in the experiment, where the control parameter is  $\alpha_0$ , the bromate feed rate. (b) Bifurcation sequence for the model, where the control parameter is  $A_0$ , the bromate feed concentration. The observed spatiotemporal patterns are steady (S), periodic (P), quasi-periodic (QP), frequency locked, period doubled (PD), and chaotic (C); some attractors corresponding to these states are illustrated in Fig. 3. Frequency-locked states are labeled by the frequency-locking ratio, except for a region labeled L in (b), where there are many different frequency-locked states, and the hatched vertical lines in (b), which are very narrow windows of frequency-locked states.

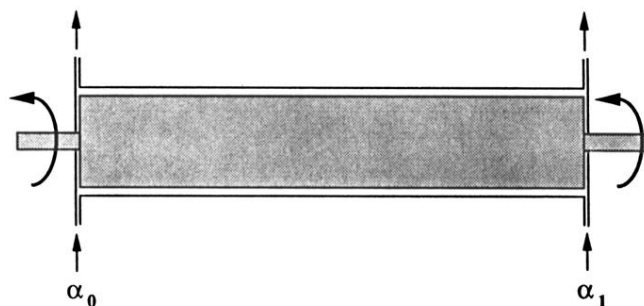


FIG. 2. The concentric-cylinder Couette reactor was mounted horizontally in a temperature-controlled bath ( $26.5 \pm 0.5^\circ\text{C}$ ). The inner (outer) cylinder radius was 1.093 cm (1.270 cm); the annulus length was 14.434 cm, which gave a fluid-height-to-gap ratio of 81.5. The bifurcation sequence was studied by varying the feed rate at  $z=0$ ,  $\alpha_0$ , from 0 to 35 ml/h; the feed contained 0.02M  $\text{KBrO}_3$  and 1.0M  $\text{H}_2\text{SO}_4$ . The feed rate at  $z=1$ ,  $\alpha_1$ , was fixed (10 ml/h); that feed contained 0.1M glucose, 0.06M acetone, 0.002M  $\text{MnSO}_4$ , and 1.0M  $\text{H}_2\text{SO}_4$ . The concentration of one of the intermediate species, bromide ion, was measured with sixteen ion-selective electrodes (Ag-AgBr) spaced equally along the axial extent of the reactor.